

# Continuous photodetection model: quantum jump engineering and hints for experimental verification

A. V. Dodonov,<sup>1,\*</sup> S. S. Mizrahi,<sup>1,†</sup> and V. V. Dodonov<sup>2,‡</sup>

<sup>1</sup>*Departamento de Física, CCET, Universidade Federal de São Carlos,  
Via Washington Luiz km 235, 13565-905, São Carlos, SP, Brazil*

<sup>2</sup>*Instituto de Física, Universidade de Brasília, PO Box 04455, 70910-900, Brasília, DF, Brazil*  
(Dated: August 31, 2018)

We examine some aspects of the continuous photodetection model for photocounting processes in cavities. First, we work out a microscopic model that describes the field-detector interaction and deduce a general expression for the Quantum Jump Superoperator (QJS), that shapes the detector's post-action on the field upon a detection. We show that in particular cases our model recovers the QJSs previously proposed ad hoc in the literature and point out that by adjusting the detector parameters one can engineer QJSs. Then we set up schemes for experimental verification of the model. By taking into account the ubiquitous non-idealities, we show that by measuring the lower photocount moments and the mean waiting time one can check which QJS better describes the photocounting phenomenon.

PACS numbers: 03.65.Ta, 42.50.Lc, 03.65.Yz, 42.50.Ct, 85.60.Gz

## I. INTRODUCTION

The subject of quantum measurements is as old as the very foundation of quantum mechanics. For a long time the scheme of sudden state reduction, proposed by von Neumann, has been prevalent. He conjectured that the measurement of an observable on a system entails its state reduction to one of its eigenstates, or shortly, a sudden change of the system state by projection. However, on probing an electromagnetic (EM) field state through a photocount process, the photons are detected and counted one by one, a photon entering a photomultiplier tube provokes a burst of electrons (a photocurrent) which is viewed as originating from that single photon. It is then registered and counted. A sequence of bursts in a given time interval is associated to the photocount process. So, the determination of the field state is not achieved by an instantaneous projective measurement, but it takes some time  $t$  to count a sequence of photons, whose statistics gives information about the field state. A classical theory describing this process was proposed by Mandel [1]. Quantum photocount theories were developed by several authors [2, 3, 4, 5, 6] (see the review [7] for more references). These theories rely on the assumption of an instantaneous measurement of  $m$  photons, independently of the duration of the detection. However, actually, photons are counted sequentially, one by one, and the time intervals between counts is irregular and uncontrollable.

For describing more realistically a sequential photocount events in an ideal closed cavity, Srinivas and Davies (SD) [8] proposed an approach based on the concept of continuous measurement. Their scheme allows calculating various statistical functions, that can be compared with experimental outcomes, such as the probability for counting any number  $k$  of photons in a time interval  $t$  and different coincidence probability densities. The SD model takes into account a “back action” of the photodetector on the state of field and gives the conditioned field state, i.e., the field state just after a given sequence of photocounting events. A progress in understanding the physical meaning of the axiomatic SD model was achieved due to studies [9, 10, 11, 12, 13] (for other references see [7, 14]).

Continuous photodetection model (CPM) is extensively discussed in the literature [7, 9, 11, 15, 16], so we shall mention only its main properties. The model, also referred as a theory, describes the field state evolution during the photodetection process in a closed cavity and is formulated in terms of two fundamental *operations*, assumed to represent the *only* events occurring at each infinitesimal time interval. (1) The one-count operation, represented by the *Quantum Jump Superoperator* (QJS), describes the detector's back-action on the field upon a single count, and the trace calculation over the QJS gives the probability per unit time for occurrence of a detection. (2) The *no-count* operation describes the field non-unitary evolution in absence of counts.

---

\*Electronic address: adodonov@df.ufscar.br

†Electronic address: salomon@df.ufscar.br

‡Electronic address: vdodonov@fis.unb.br

If one sets the formal expressions for these operations, all possible outcomes of a photocounting experiment can be predicted. For instance, the photocounts [8, 10, 11] and the waiting time (WT) [17, 18, 19, 20] statistics are among the most common quantities studied both theoretically and experimentally. Moreover, CPM conferred a new step in photodetection theories by allowing one to determine the field state after an arbitrary sequence of measurements, thus creating the possibility of controlling the field properties in real time experiments [26, 28, 53].

Actually, the QJS is the main formal ingredient within the theory, since it also dictates the form of the no-count superoperator [8]. Two different models for the QJS were proposed *ad hoc*. The first was proposed by Srinivas and Davies (SD) in the original paper [8] (we call it *SD-model*) as

$$\hat{J}_{SD}\rho = \mathcal{R}\hat{a}\hat{a}^\dagger, \quad (1)$$

where  $\rho$  is the field statistical operator,  $\hat{a}$  and  $\hat{a}^\dagger$  are the usual bosonic annihilation/creation operators and  $\mathcal{R}$  is roughly the detector's ideal counting rate [8, 21]. From the very beginning the authors [8] denounced the presence of some inconsistencies when  $\hat{J}_{SD}$  is employed for describing a real photodetection process, this point was also appointed in [21]. Nevertheless, this QJS is widely used in the literature [11, 13, 22, 23, 24, 25, 26, 27, 28, 29, 30, 31, 32].

The other proposal [16, 33] assumes for the QJS an expression written in terms of the ladder operators  $\hat{E}_- = (\hat{a}^\dagger\hat{a} + 1)^{-1/2}\hat{a}$  and  $\hat{E}_+ = \hat{E}_-^\dagger$  (also known as *exponential phase operators* [34, 35, 36, 37, 38])

$$\hat{J}_E\rho = \mathcal{R}\hat{E}_-\rho\hat{E}_+. \quad (2)$$

In [21] we called *E-model* such a choice, to distinguish it from the SD QJS (1). We note that  $\mathcal{R}$  may be different for SD- and E- models, but the above notation will not cause confusion in this paper. Besides eliminating the inconsistencies within the SD-model, the use of the E-model leads to different qualitative and quantitative predictions for several observable quantities.

In section II we present a microscopic model for the detector assumed to be composed of a sensor (2-level quantum object) and an amplification mechanism (macroscopic thermal reservoir). In section III we compare our model's predictions concerning photodetector properties with experimental data and show that the QJSs (1) and (2) are particular cases of a general time-dependent *transition superoperator*, each one occurring in a particular regime of the detector experimental parameters [39, 40]. Moreover, we point out that by manipulating detector's parameters one could engineer the form of the QJS, thus changing the dynamics of the photodetection, as well as the field state after a sequence of measurements.

A way to check the validity of CPM and to decide which QJS better describes the phenomenon in practice can be accomplished through photodetection experiments in a high finesse cavity by comparing experimental outcomes with theoretical predictions. However, real detectors and cavities are far from ideal. So in section IV we include the main non-idealities [quantum efficiency (QE) and dark counts] into the CPM and deduce general expressions for the photocounts and the WT distributions. As a practical application, in section V we give some experimental hints to decide which QJS model actually prevails in a photodetection experiment. Section VI contains a summary and the conclusions.

## II. MICROSCOPIC MODEL OF 2-LEVEL PHOTODETECTOR

We model the photodetector as constituted of two parts: the sensor and the amplification mechanism (AM). The sensor is a two-level quantum object (atom-like) with resonant frequency  $\omega_0$ , interacting with the monomodal EM field of frequency  $\omega$ . It has the ground  $|g\rangle$  and the excited  $|e\rangle$  states, so we describe it by the usual Jaynes–Cummings Hamiltonian [41]

$$H_0 = \frac{1}{2}\omega_0\sigma_0 + \omega\hat{n} + \hat{a}\hat{a}^\dagger\sigma_+ + g^*\hat{a}^\dagger\sigma_-, \quad (3)$$

where  $g$  (assumed to be real, since only its absolute value enters the final expressions) is the sensor-field coupling constant, and the sensor operators are  $\sigma_0 = |e\rangle\langle e| - |g\rangle\langle g|$ ,  $\sigma_+ = |e\rangle\langle g|$  and  $\sigma_- = |g\rangle\langle e|$ . The interaction described by Hamiltonian (3) allows a coherent exchange of excitations between the sensor and the field – the Rabi oscillations.

Upon absorbing a photon the sensor initially in  $|g\rangle$  makes a transition to  $|e\rangle$ , and after some time it decays back, emitting a *photoelectron* into the AM; after that, the detector is ready for the next photodetection. The AM is a complex macroscopic structure (e.g. photomultiplier tube) that somehow amplifies the photoelectron and originates some observable macroscopic effect, giving rise to the click of the detector. In order to describe general features of the AM independent of the type of the single photon detector (SPD), we model it as a macroscopic thermal reservoir with a mean number of intrinsic excitations  $\bar{n}$  (due to the effects of temperature and internal defects). Thus, the

whole system field-SPD unconditioned time evolution (when the detector is not monitored [14]) is described by the master equation [40]

$$\begin{aligned}\dot{\rho}_T = & \frac{1}{i} [H_0, \rho_T] - \gamma \bar{n} (\sigma_- \sigma_+ \rho_T - 2\sigma_+ \rho_T \sigma_- + \rho_T \sigma_- \sigma_+) \\ & - \gamma (\bar{n} + 1) (\sigma_+ \sigma_- \rho_T - 2\sigma_- \rho_T \sigma_+ + \rho_T \sigma_+ \sigma_-),\end{aligned}\quad (4)$$

where  $\gamma$  is the sensor-AM coupling constant.

According to CPM, the trace of QJS applied on the field density operator gives the probability density  $p(t)$  for the photodetection, i.e. emission of a photoelectron at time  $t$ , given that at time  $t = 0$  the detector-field system was in the state

$$\rho_0 = |g\rangle\langle g| \otimes \rho, \quad (5)$$

where  $\rho$  is the field statistical operator. Microscopically this means that initially the detector is in the ground state; then, during the time interval  $(0, t)$  the sensor interacted with the field and it could have absorbed a photon, doing a transition  $|g\rangle \rightarrow |e\rangle$ . So  $p(t)\Delta t$  is the probability of the sensor decaying back to  $|g\rangle$  during the time interval  $(t, t + \Delta t)$  and simultaneously emitting a photoelectron that will lately originate one click. Here, the emission of the photoelectron is our interpretation of how the detector operates, and this phenomenon does not appear explicitly in the formalism.

Following the quantum trajectories approach [14],  $p(t)$  is calculated as

$$p(t) = \text{Tr}_{F-D} [\hat{R} \hat{U}_t \rho_0], \quad (6)$$

where  $\hat{U}_t \rho_0$  represents the evolution of the field-SPD system from initial state  $\rho_0$  at time  $t = 0$  to the time  $t$  without detections, and  $\hat{R} \hat{U}_t \rho_0$  stays for a click (instantaneous decay of the sensor) at the time  $t$  (in the trace, F stands for the field and D – for the detector). The sensor instantaneous decay  $|e\rangle \rightarrow |g\rangle$  is represented by the superoperator

$$\hat{R} \rho_0 = 2\gamma (\bar{n} + 1) \sigma_- \rho_0 \sigma_+, \quad (7)$$

whose trace gives the probability density of such an event. In Eq. (7)  $\gamma$  stands for the sensor zero-temperature decay rate, and we included the term  $\bar{n} + 1$  because it is natural to assume that the rate of decays is proportional to the effective temperature of the detector (proportional to  $\bar{n}$ ). The complementary no-decay superoperator  $\hat{U}_t \rho_0 = \rho_U(t)$  describes the non-unitary evolution of the field-SPD system during time interval  $(0, t)$  without clicks; it is the solution to the master equation (4) without the decay term (7):

$$\frac{d\rho_U}{dt} = -i(H_e \rho_U - \rho_U H_e^\dagger) + 2\gamma \bar{n} \sigma_+ \rho_U \sigma_-, \quad (8)$$

where

$$H_e = \frac{(\omega_0 - i\gamma)}{2} \sigma_0 + \omega \hat{n} + g \hat{a} \sigma_+ + g \hat{a}^\dagger \sigma_- - i\gamma (\bar{n} + \frac{1}{2}). \quad (9)$$

Taking the partial trace over the detector variables in (6) one obtains the superoperator

$$\hat{\Xi}(t) \rho = \text{Tr}_D [\hat{R} \hat{U}_t \rho_0], \quad (10)$$

which describes the back-action of the detector on the field upon one click – it is the *transition superoperator* [39] and, as will be seen below, its time average defines the QJS. Moreover, the probability density for a count is simply  $p(t) = \text{Tr} [\Xi(t) \rho]$ .

In order to solve Eq. (8) we first do the transformation

$$\rho_U = X_t \tilde{\rho}_U X_t^\dagger, \quad X_t \equiv \exp(-iH_e t) \quad (11)$$

to obtain a simple equation for  $\tilde{\rho}_U$

$$\frac{d\tilde{\rho}_U}{dt} = 2\gamma \bar{n} \tilde{\sigma}_+ \tilde{\rho}_U \tilde{\sigma}_-, \quad \tilde{\sigma}_+ = X_{-t} \sigma_+ X_t, \quad \tilde{\sigma}_- = \tilde{\sigma}_+^\dagger, \quad (12)$$

whose formal solution is

$$\tilde{\rho}_U(t) = \rho_0 + 2\gamma\bar{n} \int_0^t dt' \tilde{\sigma}_+(t') \tilde{\rho}_U(t') \tilde{\sigma}_-(t'). \quad (13)$$

If one iterates Eq. (13) and substitutes the result into Eq. (10) one gets the following transition superoperator

$$\hat{\Xi}(t)\rho = 2bg(1+\bar{n}) \sum_{l=0}^{\infty} (2\gamma\bar{n})^l \hat{\Xi}_l(t)\rho, \quad (14)$$

where

$$b \equiv \gamma/g, \quad \hat{\Xi}_0(t)\rho = \hat{\theta}_0 \rho \hat{\theta}_0^\dagger, \quad \hat{\theta}_0(t) = \langle e | X_t | g \rangle. \quad (15)$$

For  $l > 0$

$$\hat{\Xi}_l(t)\rho = \int_0^t dt_1 \cdots \int_0^{t_{l-1}} dt_l \hat{\theta}_l \rho \hat{\theta}_l^\dagger, \quad \hat{\theta}_l(t, t_1, \dots, t_l) = \langle e | X_t \tilde{\sigma}_+(t_1) \tilde{\sigma}_+(t_2) \cdots \tilde{\sigma}_+(t_l) | g \rangle. \quad (16)$$

As shown in [40] it is enough to evaluate just the three initial terms in the sum (14), whose constituents are found to be

$$\begin{aligned} \hat{\theta}_0 &= -ie^{-\gamma t(\bar{n}+1/2)-i\omega(\hat{n}+1/2)t} S_{\hat{n}+1}(t) \hat{a}, & \hat{\theta}_1 &= e^{-\gamma t(\bar{n}+1/2)-i\omega\hat{n}t} \chi_{\hat{n}+1}(t-t_1) \chi_{\hat{n}}(-t_1), \\ \hat{\theta}_2 &= -ie^{-\gamma t(\bar{n}+1/2)-i\omega(\hat{n}-1/2)t} \chi_{\hat{n}+1}(t-t_1) S_{\hat{n}}(t_1-t_2) \chi_{\hat{n}-1}(-t_2) \hat{a}^\dagger, \end{aligned}$$

where

$$C_{\hat{n}}(t) = \cos(\gamma t B_{\hat{n}}/b), \quad S_{\hat{n}}(t) = \sin(\gamma t B_{\hat{n}}/b)/B_{\hat{n}}, \quad \chi_{\hat{n}} = e^{-i\omega t/2} [C_{\hat{n}}(t) - i\delta S_{\hat{n}}(t)], \quad (17)$$

$$B_{\hat{n}} = \sqrt{\hat{n} + \delta^2}, \quad \delta = (q - ib)/2, \quad q \equiv (\omega_0 - \omega)/g. \quad (18)$$

Substituting these expressions into Eq. (14), the transition superoperator turns out to be time-dependent, contrary to the standard definition of the QJS. So we evaluate the QJS as the time average of  $\hat{\Xi}(t)$  over the time interval  $T$  (to be determined later) during which the photoelectron is emitted with high probability

$$\hat{J}\rho \equiv \frac{1}{T} \int_0^T dt \hat{\Xi}(t)\rho. \quad (19)$$

Considering the weak coupling ( $\omega, \omega_0 \gg \gamma, g$ ) for which the Jaynes–Cummings Hamiltonian (3) and the master equation (4) are valid, and expressing the field density operator in Fock basis as

$$\rho = \sum_{m,n=0}^{\infty} \rho_{mn} |m\rangle \langle n|, \quad (20)$$

after the averaging in (19) the off-diagonal elements of  $\hat{J}\rho$  vanish due to rapid oscillations of the terms  $\exp(\pm i\omega t)$ . Therefore, we are left only with the diagonal elements of  $\hat{J}\rho$ . Applying the superoperators  $\hat{\Xi}_l$  on the density matrix as in (14) and evaluating Eq. (19) we obtain

$$\hat{J}\rho = \sum_{n=0}^{\infty} \rho_{nn} \left[ n J_n^{(B)} |n-1\rangle \langle n-1| + J_n^{(D)} |n\rangle \langle n| + (n+1) J_n^{(E)} |n+1\rangle \langle n+1| + \cdots \right], \quad (21)$$

where the explicit expressions for the  $n$ -dependent functions  $J_n^{(B)}$ ,  $J_n^{(D)}$  and  $J_n^{(E)}$  are given in [40].

The QJS (21) contains an infinite number of terms, so after a click the initial field state  $\rho$  reduces to a mixture of different states, each one with its respective probability. The first term, with coefficient  $J_n^{(B)}$ , takes out a photon from the field, so it represents a click preceded by a photoabsorption – we call this event a “bright count”. The second term, dependent on  $J_n^{(D)}$  (proportional to  $\bar{n}$ , quite small as will be shown below), does not subtract photons from the field but only modifies the relative weight of the field state components – it represents a “dark count”, when the detector emits a click due to the amplification of its intrinsic excitations. All further terms in Eq. (21) are proportional to  $\bar{n}^l$ ,  $l \geq 2$ ; they describe emissions of several photons into the field upon a click, so we call the first of these terms,  $J_n^{(E)}$ , the “emission term”. There are many different phenomena that give rise to dark counts [42, 43, 44], our model takes into account only those causing the sensor’s ground–excited state transition. Since the sensor’s state depends on its interaction with the field, the dark counts modify indirectly the relative weight between the field state components – that is why they depend on  $n$ , what is not obvious at first glance.

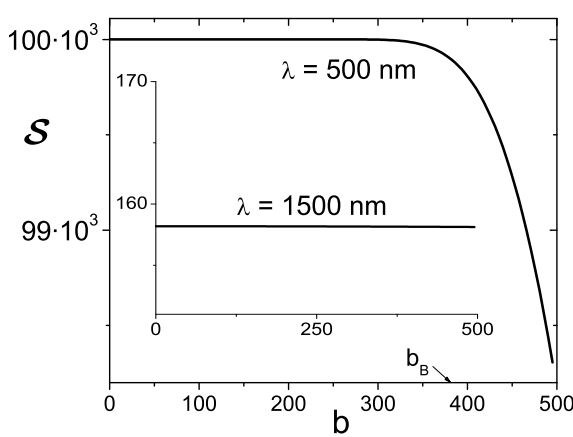


FIG. 1: Signal-to-Noise ratio as function of  $b$  at resonance ( $\lambda = 500$  nm) and far from it ( $\lambda = 1500$  nm) in the inset. The estimated breakdown value is  $b_B \approx 380$ .

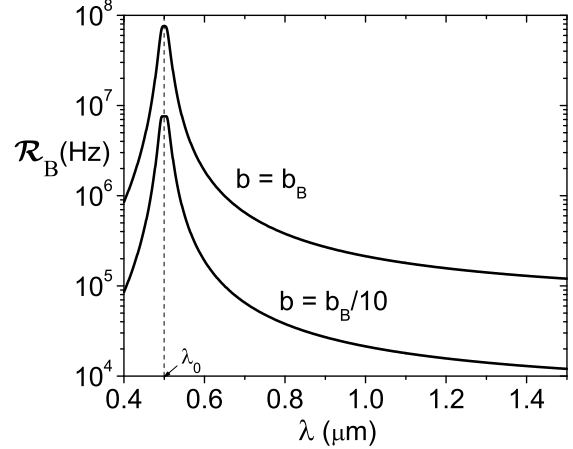


FIG. 2: Bright counts rate as function of wavelength of the field for different values of  $b$ , showing that  $\mathcal{R}_B$  increases proportionally to  $b$ . The resonant wavelength is  $\lambda_0 = 500$  nm.

### III. COMPARISON TO EXPERIMENTAL DATA AND QJS ENGINEERING

Now we compare our results regarding SPD properties with available experimental data. Experimentally [46] the dependencies of bright and dark counts rates are set as functions of the light wavelength and the detector's "bias parameter" (BP). In the BP we englobe such quantities as bias voltage, bias current and other physical quantities the experimenter adjusts in order to achieve simultaneously the highest Signal-to-Noise ratio  $\mathcal{S}$  and bright counts rate.  $\mathcal{S} \equiv \mathcal{R}_B/\mathcal{R}_D$  is the ratio between the bright,  $\mathcal{R}_B$ , and dark,  $\mathcal{R}_D$ , counts rates. When one increases the BP, the bright counts rate increases while  $\mathcal{S}$  remains unchanged until the *breakdown* value of BP, when  $\mathcal{S}$  starts to fall rapidly as function of the BP. So most detectors usually operate near the BP breakdown in order to achieve the optimal performance. In practice,  $\mathcal{R}_B$  is determined by directing laser pulses containing in average one photon at a given repetition rate on the detector and measuring the rate of counts, so in our model it is described by the term  $J_1^{(B)}$ . Analogously,  $\mathcal{R}_D$  is calculated as the rate of counts in the absence of any input signal, so it is given by  $J_0^{(D)}$ .

To do the comparison we need to set the values for our model free parameters:  $\omega_0$ ,  $g$ ,  $\Upsilon = \gamma T$  and  $\bar{n}$ . For simplicity we shall express the frequencies  $\omega_0$  and  $\omega$  in terms of respective wavelengths  $\lambda_0$  and  $\lambda$ . Thus we are left with two parameters,  $\lambda$  and  $b$ , where  $b$  plays the role of the BP. Our general model cannot determine the  $\text{BP} \times b$  dependence for every kind of detector; nevertheless, one may argue that the BP and  $b$  must be proportional to each other, since for zero BP one should also have  $b = 0$ , because in this case the detector would be turned off. Here, we do not need to know the exact dependence of the BP on  $b$  provided we determine the breakdown value  $b_B$ , corresponding to the BP breakdown at resonance, and take it as a measure of  $b$ .

After numerical simulations we have chosen values of the free parameters that reproduce qualitatively the common experimental behavior [43, 45, 46, 47] and lie within the applicability region of the model:  $\lambda_0 = 500$  nm,  $g = 10^{11}$  Hz,  $\Upsilon = 5 \times 10^5$  and  $\bar{n} = 10^{-11}$ , so  $b_B \approx 380$ , as shown in figure 1. Moreover, we verified that below  $b_B$  both  $\mathcal{R}_B$  and  $\mathcal{R}_D$  have approximately linear dependence on  $b$ , in agreement with our qualitative arguments. In figure 2 we plot  $\mathcal{R}_B$  for two different values of  $b$  as function of the light wavelength, where we see a good agreement with experimental results [45] and can check that  $\mathcal{R}_B$  is proportional to  $b$ . We also confirmed numerically that  $\mathcal{R}_D$  does not depend on the field wavelength, as expected.

We verified that for the chosen parameters the emission terms [ $J_n^{(E)}$  and further terms in Eq. (21)] are at least 10 orders of magnitude smaller than the dark counts term and even more for bright counts term in Eq. (21). This confirms that detectors do not emit photons into the field. Intuitively, the emission of photons by the detector would be possible only at temperatures much higher than room temperature through black body radiation, which is not the case in experiments. Thus, in practice one is dealing only with bright and dark counts terms that act on the field simultaneously every time a count is registered, so the QJS takes the form

$$\hat{J}\rho = \text{diag} \left[ \left( \hat{J}_B + \hat{J}_D \right) \rho \right], \quad (22)$$

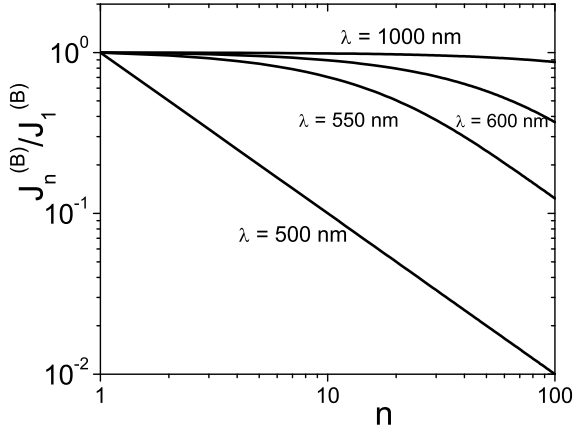


FIG. 3: Normalized bright counts term as function of  $n$  in di-log scale at breakdown  $b_B$ . At resonance ( $\lambda = 500$  nm) we have  $\beta \approx 1/2$  and far away from resonance ( $\lambda = 1000$  nm)  $\beta \approx 0$  [see Eq. (24)].

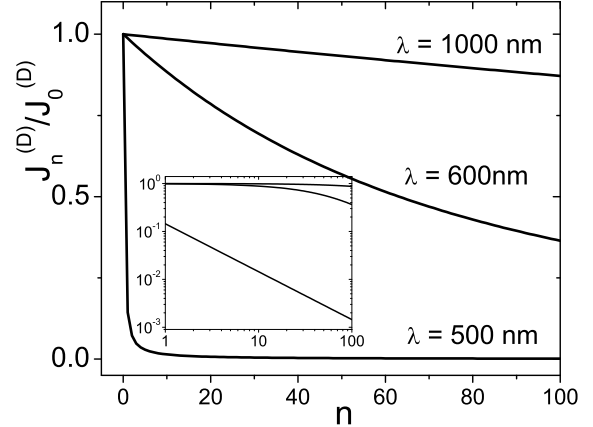


FIG. 4: Normalized dark counts term as function of  $n$  at breakdown  $b_B$  for different field wavelengths and the same graph in di-log scale in the inset.

where diag means diagonal terms in Fock basis. In figure 3 we show the dependence of the normalized bright counts term  $J_n^{(B)}/J_1^{(B)}$  on  $n$  in di-log scale (for better visualization we joined the points). We note that near and far away from resonance – see the values of  $\lambda$  in the caption – one has nearly polynomial dependence (linear in di-log scale)

$$J_n^{(B)} \approx J_1^{(B)} n^{-2\beta} = \mathcal{R}_B n^{-2\beta} \quad (23)$$

with  $\beta \approx 1/2$  at resonance and  $\beta \approx 0$  far away from it. Thus, in these cases one can write the operator dependence of bright counts as

$$\hat{J}_B \rho = \mathcal{R}_B (\hat{n} + 1)^{-\beta} \hat{a} \rho \hat{a}^\dagger (\hat{n} + 1)^{-\beta}, \quad (24)$$

thus recovering the E-model with  $\beta \approx 1/2$  at the resonance and SD-model with  $\beta \approx 0$  far away from it, although the values of  $\mathcal{R}_B$  are different in each case (see figure 2).

The normalized dark counts term  $J_n^{(D)}/J_0^{(D)}$  is shown in figure 4 in linear scale and in di-log scale in the inset. Out of resonance  $J_n^{(D)}$  is almost independent on  $n$ , so in this case  $J_n^{(D)} \approx \mathcal{R}_D = \text{const}$ . At the resonance, for  $n = 0$  one gets  $J_0^{(D)} = \mathcal{R}_D$  and for  $n > 0$  we have  $J_{n>0}^{(D)} \approx \xi \cdot \mathcal{R}_D \cdot n^{-2\beta}$ , where  $\beta \approx 1/2$  and  $\xi$  is a number less than 1 ( $\mathcal{R}_D$  does not depend on the wavelength). This means that at resonance the dark counts are suppressed in the presence of light. This happens because they occur when the detector in the ground state is excited by its intrinsic processes; however, at resonance the rate of excitations by photons from the field is much higher than by intrinsic processes, so the dark counts “have no time” to appear. Therefore, the operator form of the dark counts term in Eq. (21) is

$$\hat{J}_D \rho = \mathcal{R}_D [\Lambda_0 \rho \Lambda_0 + \xi \Lambda \hat{n}^{-\beta} \rho \hat{n}^{-\beta} \Lambda], \quad (25)$$

where  $\Lambda_0 \equiv |0\rangle\langle 0|$ ,  $\Lambda \equiv 1 - \Lambda_0$  and at resonance we have the E-model with  $\beta \approx 1/2$  and  $\xi < 1$ . Far away from resonance we recover the SD-model with  $\beta \approx 0$  and  $\xi = 1$ .

Thus we have exposed our microscopic model for the photodetector and showed that when one is concerned about the photodetector behavior, the model agrees with experimental data. Still, the only way to verify whether the formal expressions of QJSs resulting from the model hold in practice is to perform photocounting experiments and compare the outcomes, such as photocounts or WT distributions, to the model’s prediction. In the next sections we shall treat this issue for realistic situations of detectors with non-unit quantum efficiency and non-zero dark counts rate. We also discuss possible measurements that may permit to discern between the E-model and the SD-model, even in the presence of low efficiency and dark counts.

#### IV. INCLUDING THE NON-IDEALITIES

We consider a model for a photodetector with non-unit quantum efficiency (QE) and a finite dark counts rate. In [48] we have also considered the effects associated to cavity damping and the detector's dead-time, and showed that they are not crucial when compared to the QE and dark counts. Moreover, as the QJS (1) is an unbounded superoperator, the inclusion of dead-time effect into the CPM leads to some inconsistencies within SD-model, such as non-normalizable photodetection distribution. On the other hand, the E-model is free from such problems.

##### A. SD-model

We consider a free electromagnetic monomodal field of frequency  $\omega$ , enclosed in an ideal cavity together with a photodetector. The *unconditioned time evolution* (UTE) of the field in the presence of the detector, i.e. the evolution when the detector is turned on but the outcomes of the measurements are disregarded (not registered), is described by the master equation [9, 16, 24]

$$\dot{\rho} = -i\omega(\hat{n}\rho - \rho\hat{n}) - \frac{\mathcal{R}}{2}(\hat{n}\rho + \rho\hat{n} - 2\hat{A}\rho), \quad \hat{A}\rho \equiv \hat{a}\rho\hat{a}^\dagger, \quad \hat{n} = \hat{a}^\dagger\hat{a}. \quad (26)$$

The first term on the RHS stands for the free field evolution and the second describes the effect of the detector on the field due to their mutual interaction. The parameter  $\mathcal{R} \equiv \mathcal{R}_B$  (we omit the subscript  $B$  to simplify the notation) is the field-detector coupling constant, roughly equal to the ideal counting rate.

To describe photodetection with QE  $\eta$  and the dark counts rate  $\mathcal{R}d$  ( $d$  is the ratio between the dark counts rate and the ideal photon counting rate), we take  $\beta = 0$  and  $\xi = 1$  in Eq. (25)

$$\hat{J}\rho = \mathcal{R}(\eta\hat{A} + d)\rho. \quad (27)$$

The first term within the parenthesis describes the absorption of a photon from the field with probability per unit time  $\text{Tr}[\eta\mathcal{R}\hat{A}\rho] = \eta\mathcal{R}\bar{n}$ , where  $\bar{n}$  is the field mean photon number – this means that the detector “sees” all the photons. The second term describes the dark counts, so after a detector's click the field state becomes a mixture of two possible outcomes: either a photon absorption or a dark count.

The no-count state  $\rho_S \equiv \hat{S}_t\rho_0$ , where  $\hat{S}_t$  is the no-count superoperator, obeys Eq. (26) when one subtracts the term (27) on the RHS (see [14, 49]). Moreover, as we are interested in calculating probabilities, we shall disregard phase factors  $\exp(\pm i\omega\hat{n}t)$ , since they are canceled in the trace calculation. So the evolution equation of  $\rho_S$  is

$$\dot{\rho}_S = -\frac{\mathcal{R}}{2}(\hat{n}\rho_S + \rho_S\hat{n}) + \mathcal{R}v\hat{A}\rho_S - \mathcal{R}d\rho_S, \quad v \equiv 1 - \eta. \quad (28)$$

We solved this equation in [48], obtaining

$$\hat{S}_t\rho_0 = e^{-d\mathcal{R}t}\hat{E}_t(e^{v\phi_t\hat{A}}\rho_0), \quad \hat{E}_t\rho = e^{-\mathcal{R}\hat{n}t/2}\rho e^{-\mathcal{R}\hat{n}t/2}, \quad \phi_t = 1 - e^{-\mathcal{R}t}. \quad (29)$$

The field UTE superoperator  $\hat{T}_t$ , defined as the solution to Eq. (26), is naturally given by setting  $d = \eta = 0$  in Eqs. (28) and (29). We introduced in Eq. (29) a compact notation for the infinite sum in terms of the exponential superoperator:

$$\exp(v\phi_t\hat{A})\rho_0 \equiv \sum_{l=0}^{\infty} \frac{(v\phi_t)^l}{l!} \hat{a}^l \rho_0 (\hat{a}^\dagger)^l. \quad (30)$$

The  $m$ -counts superoperator  $\hat{N}_t(m)$ , that describes the field state after  $m$  registered counts (whatever real or dark ones) in the time interval  $(0, t)$ , and whose trace gives the probability for this event is

$$\hat{N}_t(m)\rho = \int_0^t dt_m \int_0^{t_m} dt_{m-1} \cdots \int_0^{t_2} dt_1 \hat{S}_{t-t_m} \hat{J} \hat{S}_{t_m-t_{m-1}} \hat{J} \cdots \hat{J} \hat{S}_{t_1} \rho, \quad (31)$$

and after some manipulations [48] it reduces to

$$\hat{N}_t(m) = \hat{S}_t \frac{(d\mathcal{R}t + \eta\phi_t\hat{A})^m}{m!}. \quad (32)$$

A simple manner for contrasting the predictions of the model to the experimental data is by looking to the lower photocounts moments

$$\bar{m}_t = \sum_{m=0}^{\infty} m \text{Tr} \left[ \hat{N}_t(m) \rho_0 \right] = d\mathcal{R}t + \eta \bar{n} \phi_t \quad (33)$$

$$\overline{m(m-1)}_t = (d\mathcal{R}t)^2 + 2\eta \bar{n} d\mathcal{R}t \phi_t + (\eta \phi_t)^2 \overline{n(n-1)}, \quad (34)$$

where  $\bar{n}$  and  $\overline{n(n-1)}$  are the factorial moments of the initial density operator.

Another measurable quantity we consider is the *waiting time distribution*. It describes the probability density for registering two consecutive clicks separated by the time interval  $\tau$ , provided the first one occurred at time  $t$ . Its non-normalized form is

$$W_t(\tau) = \text{Tr} \left[ \hat{J} \hat{S}_\tau \hat{J} \hat{T}_t \rho \right], \quad (35)$$

and the mean WT is

$$\bar{\tau} = \mathcal{N}^{-1} \int_0^\theta d\tau W_t(\tau) \tau, \quad \mathcal{N} = \int_0^\theta d\tau W_t(\tau), \quad (36)$$

where  $\theta$  is the time interval during which one evaluates the averaging in experiments. As to be shown in section V,  $\theta$  is an important parameter due to the presence of dark counts. We obtained the expression for  $W_t(\tau)$  in [48]:

$$W_t(\tau) = e^{-d\mathcal{R}\tau} \left\{ \eta^2 e^{-\mathcal{R}(2t+\tau)} \Phi_2^W + \eta d e^{-\mathcal{R}t} (1 + e^{-\mathcal{R}\tau}) \Phi_1^W + d^2 \Phi_0^W \right\}, \quad (37)$$

where

$$\Phi_k^W = \sum_{n=k}^{\infty} \rho_n \frac{n!}{(n-k)!} (1 - \eta \phi_\tau e^{-\mathcal{R}t})^{n-k}, \quad \rho_n = \langle n | \rho | n \rangle. \quad (38)$$

## B. E-model

We now repeat the same procedures for the E-model with the QJS

$$\hat{J}\rho = \mathcal{R}(\eta \hat{\varepsilon} + d)\rho, \quad \hat{\varepsilon}\rho \equiv \hat{E}_- \rho \hat{E}_+. \quad (39)$$

For simplicity we considered a simplified form for the dark counts term, analogous to the one we used in SD-model, but different from the one given by Eq. (25). The probability per unit time for detecting a photon is  $\eta \mathcal{R}(1 - p_0)$ , where  $p_0 = \langle 0 | \rho | 0 \rangle$ , so the detector “sees” whether there is a photon in the cavity. In principle, the parameter  $\mathcal{R}$  is different from the one in SD-model, but here it will be always clear which one we are dealing with. The field UTE is described by an equation similar to Eq. (26), obtained by doing the substitution  $\{\hat{a}, \hat{a}^\dagger\} \rightarrow \{\hat{E}_-, \hat{E}_+\}$  in the non-unitary evolution [second term on the RHS of Eq. (26)]. So the no-count state  $\rho_S$  obeys the equation

$$\dot{\rho}_S = -\frac{\mathcal{R}}{2} \left( \hat{\Lambda} \rho_S + \rho_S \hat{\Lambda} \right) + \mathcal{R} v \hat{\varepsilon} \rho_S - d \mathcal{R} \rho_S, \quad (40)$$

[similar to Eq. (28)] where  $\hat{\Lambda} \equiv \hat{E}_+ \hat{E}_- = 1 - \hat{\Lambda}_0$ ,  $\hat{\Lambda}_0 \equiv |0\rangle\langle 0|$ . Since we are going to calculate probabilities, it is sufficient to write out just the *diagonal* form of the no-count superoperator in the Fock basis, given by [48]

$$\hat{S}_t \cdot = e^{-d\mathcal{R}t} \left[ \hat{P}_t \cdot + \hat{\Lambda}_0 \frac{1 - \hat{P}_t}{1 - v \hat{\varepsilon}} \cdot \hat{\Lambda}_0 \right], \quad \hat{P}_t \equiv e^{-\mathcal{R}t(1 - v \hat{\varepsilon})}, \quad (41)$$

where the dot  $\cdot$  stands for any density operator. Once again, the functions of the superoperator  $\hat{\varepsilon}$  should be calculated as power series.

The  $m$ -counts superoperator is

$$\begin{aligned} \hat{N}_t(m) \cdot &= e^{-d\mathcal{R}t} \left\{ \left( 1 - \hat{\Lambda}_0 \frac{1}{1-v\hat{\varepsilon}} \cdot \hat{\Lambda}_0 \right) \hat{P}_t \frac{(\hat{J}t)^m}{m!} + \hat{\Lambda}_0 \frac{1}{1-v\hat{\varepsilon}} \frac{(d\mathcal{R}t)^m}{m!} \cdot \hat{\Lambda}_0 \right. \\ &\quad \left. + \hat{\Lambda}_0 \frac{\mathcal{R}\eta\hat{\varepsilon}}{1-v\hat{\varepsilon}} \int_0^t dx \hat{P}_x \frac{[d\mathcal{R}t + \eta\hat{\varepsilon}\mathcal{R}x]^{m-1}}{(m-1)!} \cdot \hat{\Lambda}_0 \right\}, \end{aligned} \quad (42)$$

where the last term is zero for  $m = 0$ , and the expressions for the initial factorial photocounts moments read

$$\bar{m}_t = d\mathcal{R}t + \eta\bar{n}(1 - \Xi_1), \quad (43)$$

$$\overline{m(m-1)}_t = (d\mathcal{R}t)^2 + 2\eta\bar{n}d\mathcal{R}t(1 - \Xi_1) + \eta^2 \left[ \overline{n(n-1)}(1 - \Omega) - 2\bar{n}\mathcal{R}t\Xi_2 \right], \quad (44)$$

where

$$\Xi_k \equiv \frac{1}{\bar{n}} \text{Tr} \left[ \frac{\hat{\varepsilon}^k}{1-\hat{\varepsilon}} \hat{P}_t^0 \rho \right], \quad \Omega \equiv \frac{2}{n(n-1)} \text{Tr} \left[ \left( \frac{\hat{\varepsilon}}{1-\hat{\varepsilon}} \right)^2 \hat{P}_t^0 \rho \right], \quad \hat{P}_t^0 \equiv \hat{P}_t(v=1). \quad (45)$$

Using Eq. (35), the WT distribution is found to be

$$W_t(\tau) = e^{-d\mathcal{R}\tau} \left\{ (\mathcal{R}d)^2 [1 - \text{Tr}(\hat{P}_t^0 \rho)] + \text{Tr}[(\hat{J}\hat{P}_\tau + \mathcal{R}d\hat{\Lambda}_0 \frac{1-\hat{P}_\tau}{1-v\hat{\varepsilon}} \cdot \hat{\Lambda}_0) \hat{J}\hat{P}_t^0 \rho] \right\}. \quad (46)$$

## V. SOME SCHEMES FOR VERIFYING CPM

Guided by experimental data [51] we chose the following numerical values for the model parameters:  $\eta = 0.6$  for the QE and  $d = 5 \cdot 10^{-3}$  for the dark counts rate (normalized by the ideal counting rate). We do not attribute any fixed value to  $\mathcal{R}$  since our analysis will be given in terms of the dimensionless  $\mathcal{R}t$  ( $t$  being the time). As many photodetection quantities were reported in different contexts [8, 11, 15, 16, 17, 20, 21, 53], we shall consider few of them that could help to decide between the SD- or the E- model.

We first analyze the counting statistics. In figure 5 we plot  $\bar{m}_t$  as function of  $\mathcal{R}t$  for both models for two values of the initial mean photon number,  $\bar{n} = 50$  and  $100$ . Initially,  $\bar{m}_t$  increases steeply due to photons absorption, and after some time the growth turns linear with much smaller slope due to the dark counts. We call the time interval during which the photons are absorbed (representing the duration of the steep increase in the number of counts) the *effective counting time*  $t_E$ . In the E-model  $t_E$  is proportional to the initial average photon number, contrary to the SD-model [as seen from the figure 5 and formulae (33) and (43)]. So the experimental analysis of the dependence of  $t_E$  on  $\bar{n}$  seems to us a feasible way for verifying which model could hold in practice, because, according to the SD-model,  $t_E$  does not depend on  $\bar{n}$ . Moreover, one could also check the validity of each model by verifying whether  $\bar{m}_t$  depends on the initial field state: in the SD-model it is independent of the field state, while in the E-model  $\bar{m}_t$  is quite sensible to it: in figure 5 one sees a notable difference between thermal and coherent states, although not so much between number and coherent states. This can be explained by a great difference in the values of Mandel's  $Q$ -factor [52] characterizing the statistics of photons in the initial state: it equals  $-1$  and  $0$  for number and coherent states, respectively, whereas it is very big ( $Q_{th} = \bar{n}$ ) for the thermal states with big mean numbers of photons.

Now we analyze the normalized second factorial moment

$$K_t \equiv \overline{m(m-1)}_t / \bar{m}_t^2 \quad (47)$$

for the same initial states with mean photon number  $\bar{n} = 50$ . For the number and thermal states  $K_t$  as function of  $\mathcal{R}t$  is shown in figure 6, and for the coherent state we get  $K_t = 1$ , so it is not plotted. In the asymptotic time limit and for non-zero dark counts rate, the same value  $K_\infty \rightarrow 1$  holds for both models, however the transient is model dependent. In the SD-model without considering dark counts  $K_t$  is time-independent,  $K_t = n(n-1)/\bar{n}^2$  ( $\bar{n}$  and  $n(n-1)$  correspond to the initial field state), nevertheless it depends on the initial field state:  $K_t = 2$  for the thermal state and  $K_t = 1 - 1/\bar{n}$  for the number state. By including the dark counts in the analysis this constant

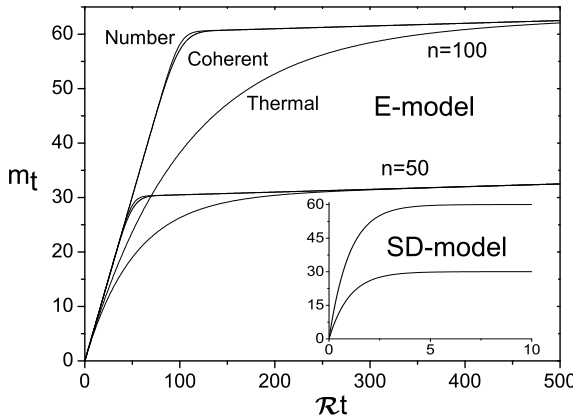


FIG. 5:  $\bar{m}_t$  in E-model for coherent, number and thermal states (indicated in the figure, the lower curves are labeled analogously) as function of time: the lower curves correspond to  $\bar{n} = 50$  and the upper – to  $\bar{n} = 100$ . In the inset we plot  $\bar{m}_t$  for the SD-model, which is independent from field state.

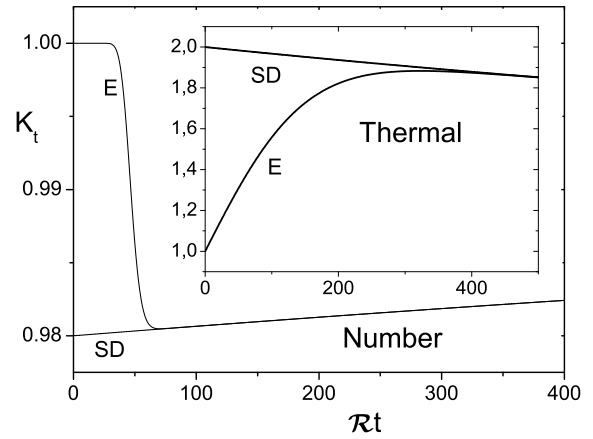


FIG. 6:  $K_t$ , Eq. (47), for SD- and E- models (as indicated in the graph with abbreviations) for the number state (and the thermal state in the inset) for  $\bar{n} = 50$ . For the coherent state one has  $K_t = 1$  at all times for both models.

behavior is slowly modified as time goes on, see figure 6. In the E-model in the absence of dark counts  $K_t$  starts at the value

$$\lim_{t \rightarrow 0} K_t = \frac{\text{Tr}(\hat{\varepsilon}^2 \rho)}{[\text{Tr}(\hat{\varepsilon} \rho)]^2} = \frac{1 - \rho_0 - \rho_1}{(1 - \rho_0)^2}, \quad (48)$$

which is exactly 1 for the number state and very close to 1 for the thermal state with the chosen values of  $\bar{n}$ . With the course of time,  $K_t$  attains the same values as for the SD-model (for respective initial field states) when all the photons have been counted. By taking in account the dark counts, such a behavior is slightly modified, yet it is quite different from the behavior in the SD-model, as shown in the figure 6. This is another possible manner for verifying the applicability of SD- or E- models.

We now turn our attention to the WT analysis. It is important to define the time interval over which we do the average: if one has non-zero dark counts rate, then by performing the average over a very large time interval, we shall always get for the mean WT the value  $\bar{\tau} \sim (\mathcal{R}d)^{-1}$ , which is nothing but the mean time interval between consecutive dark counts. Since experimentally the average is done over finite time intervals, we shall proceed in the same way: the mean WT for initial times, when the photon number is significative, is roughly  $(\eta \mathcal{R})^{-1}$  (because  $\eta \mathcal{R}$  is the effective counting rate), so we shall take the average over a time interval  $\theta = 10(\eta \mathcal{R})^{-1}$ . This means that if one does not detect consecutive counts within the time  $\theta$ , such a measurement will not contribute to the average. In an ideal case this procedure is not necessary because the probability for registering consecutive clicks separated by a large time interval is zero.

In figure 7 we plot the mean WT for the SD- and E- models, for the number and thermal initial states (for the coherent state we obtain a curve almost identical to the one for the number state) with  $\bar{n} = 100$  as function of the mean photon number in the cavity at the moment of the first click,

$$N_{CAV} = \text{Tr} \left[ \hat{n} \hat{T}_t \rho_0 \right] = \begin{cases} \bar{n} e^{-\mathcal{R}t} & \text{for SD-model} \\ \bar{n} \Xi_1 & \text{for E-model.} \end{cases} \quad (49)$$

(For completeness, in the inset of figure 7 we plot  $N_{CAV}$  as function of  $\mathcal{R}t$  for both models.) For the E-model, we see that when  $N_{CAV}$  becomes less than 1, the WT starts to increase visibly due to the dominance of dark counts, which are much more rare events than absorption of photons. This is a drastic departure from the ideal case, in which no counts occur after all the photons have been absorbed, so the mean WT saturates at the inverse value of the counting rate, as shown in [21]. Moreover, from figure 7 one verifies that as long as there are photons in the

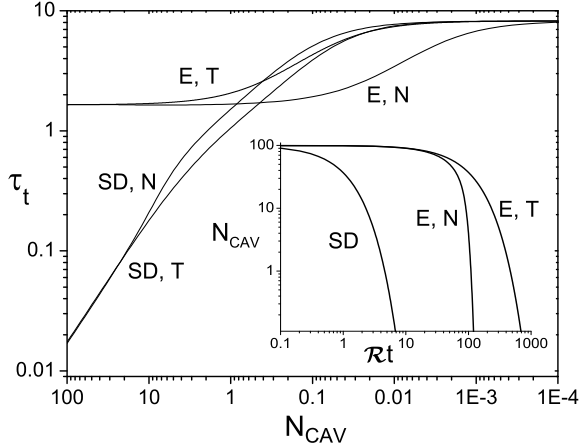


FIG. 7: Mean WT  $\bar{\tau}_t$  as function of  $N_{CAV}$  for the number (N) and thermal (T) states for SD- and E-models. While there are photons in the cavity  $\bar{\tau}_t$  is constant for the E-model, but increases substantially with time for the SD-model. In the inset we plot  $N_{CAV}$  as function of  $\mathcal{R}t$  (assuming the same  $\mathcal{R}$  for both models) for these states (in the SD-model  $N_{CAV}$  is state independent).

cavity the mean WT is nearly time-independent within the E-model (and truly independent in the ideal case [21]), and does increase substantially in time for SD-model. This is another notable qualitative difference that could be verified experimentally.

## VI. SUMMARY AND CONCLUSIONS

We presented a microscopic model for a photodetector modeled as a 2-level quantum sensor plus a macroscopic amplification mechanism. Using the quantum trajectories approach we deduced a general QJS describing the back-action of the detector on the field upon a photocount and showed that it can be represented formally as an infinite sum of terms. In that sum we have identified the terms corresponding to the bright counts (photoabsorptions), the dark counts and emission events, each one occurring with its respective probability. Adjusting the free parameters of the model to fit experimental data, we showed that the emission terms can be disregarded in realistic situations since their contribution becomes insignificant, so the QJS consists effectively only of bright and dark counts terms. Moreover, we have simulated the experimental behavior of the counting rates and the Signal-to-Noise ratio, showing the breakdown phenomenon. We have also showed that with the detector operating near its breakdown bias one can engineer the QJS by modifying the wavelength of the field. In particular, one recovers the QJSs proposed previously *ad hoc*: at resonance one gets the E-model, and far away from it the SD-model is identified.

We have also generalized the continuous photodetection model through a quantum treatment of non-ideal effects that are ubiquitous in experiments. We derived general expressions for the fundamental operations in the presence of non-unit quantum efficiency and dark counts, and calculated explicitly the photocounts and the waiting time probability distributions for initial coherent, number and thermal field states. By calculating the first and second factorial moments of the photocounts and the mean waiting time, we showed that in standard photodetection experiments one could check the applicability of the QJS of SD- or E- models. Namely, we indicated three different ways for revealing the actual QJS: (1) quantitatively, by studying the time dependence of the normalized second factorial photocounts moment. Qualitatively, we showed that the models can also be distinguished by measuring: (2) whether the effective detection time depends on the initial average photon number in the cavity and (3) whether the mean waiting time is modified as time goes on. Still, if the experimental data would depart significantly from the theoretical predictions one should reconsider both models and try to look for alternative mechanisms to reproduce the outcomes.

### Acknowledgments

Work supported by FAPESP (SP, Brazil) contract # 04/13705-3. SSM and VVD acknowledge partial financial support from CNPq (DF, Brazil).

---

[1] Mandel L 1958 *Proc. Phys. Soc.* **72** 1037

[2] Glauber R J 1963 *Phys. Rev.* **130** 2529

[3] Mandel L, Wolf E and Sudarshan E C G 1964 *Proc. Phys. Soc.* **84** 435

[4] Kelley P L and Kleiner W H 1964 *Phys. Rev.* **136** 316

[5] Mollow B R 1968 *Phys. Rev.* **168** 1896

[6] Scully M O and Lamb W E Jr *Phys. Rev.* **179** 368

[7] Peřinová V and Lukš A 2000 *Progress in Optics* **40** ed E Wolf (Amsterdam: Elsevier) pp 115

[8] Srinivas M D and Davies E B 1981 *Opt. Acta* **28** 981

[9] Milburn G J and Walls D F 1984 *Phys. Rev. A* **30** 56

[10] Ueda M 1989 *Quantum. Opt.* **1** 131

[11] Ueda M, Imoto N and Ogawa T 1990 *Phys. Rev. A* **41** 3891

[12] Imoto N, Ueda M and Ogawa T 1990 *Phys. Rev. A* **41** 4127

[13] Ueda M and Kitagawa M 1992 *Phys. Rev. Lett.* **68** 3424

[14] Carmichael H 1993 *An Open Systems Approach to Quantum Optics* (Berlin: Springer)

[15] Srinivas M D 1996 *PRA MANA - J. Phys.* **47** 1

[16] de Oliveira M C, Mizrahi S S and Dodonov V V 2003 *J. Opt. B: Quantum Semiclassical Opt.* **5** S271

[17] Ban M 1995 *Opt. Commun.* **117** 447

[18] Vyas R and Singh S 1988 *Phys. Rev. A* **38** 2423

[19] Carmichael H J, Singh S, Vyas R and Rice P R 1989 *Phys. Rev. A* **39** 1200

[20] Lee C T 1993 *Phys. Rev. A* **48** 2285

[21] Dodonov A V, Mizrahi S S and Dodonov V V 2005 *J. Opt. B: Quantum Semiclassical Opt.* **7** 99

[22] Ueda M, Imoto N and Nagaoka H 1996 *Phys. Rev. A* **53** 3808

[23] Prataviera G A and de Oliveira M C 2004 *Phys. Rev. A* **70** 011602(R)

[24] Calsamiglia S, Barnett S M, Lütkenhaus N and Suominen K -A *Phys. Rev. A* **64** 043814

[25] Saito H and Ueda M 2003 *Phys. Rev. A* **68** 043820

[26] de Oliveira M C, da Silva L F and Mizrahi S S 2002 *Phys. Rev. A* **65** 062314

[27] Peřinová V, Lukš A and Křepelka J 1996 *Phys. Rev. A* **54** 821

[28] Ban M 1995 *Phys. Rev. A* **51** 1604

[29] Ogawa T, Ueda M and Imoto N 1991 *Phys. Rev. Lett.* **66** 1046

[30] Ogawa T, Ueda M and Imoto N 1991 *Phys. Rev. A* **43** 6458

[31] Holmes C A, Milburn G J and Walls D F 1989 *Phys. Rev. A* **39** 2493

[32] Pegg D T 2006 *Phys. Rev. A* **74** 063812

[33] Ben-Aryeh Y and Brif C 1995 Discrete photodetection and Susskind-Glogower ladder operators *Preprint* quant-ph/9504009

[34] Susskind L and Glogower J 1964 *Physics* **1** 49

[35] Carruthers P and Nieto M 1968 *Rev. Mod. Phys.* **40** 411

[36] Vourdas A 1992 *Phys. Rev. A* **45** 1943

[37] Peřinová V, Lukš A and Peřina J 1998 *Phase in Optics* (Singapore: World Scientific)

[38] Wünsche A 2001 *J. Opt. B: Quantum Semiclassical Opt.* **3** 206

[39] Dodonov A V, Mizrahi S S and Dodonov V V 2005 *Phys. Rev. A* **72** 023816

[40] Dodonov A V, Mizrahi S S and Dodonov V V 2006 *Phys. Rev. A* **74** 033823

[41] Jaynes E T and Cummings F W 1963 *Proc. IEEE* **51** 89

[42] Karve G et al 2005 *Appl. Phys. Lett.* **86** 063505

[43] Kitaygorsky J et al 2005 *IEEE Trans. Appl. Superconductivity* **15** 545

[44] Panda S, Panda B K and Mishra S G 2004 *Phys. Rev. B* **69** 195304

[45] Rochas A, Gani M, Furrer B, Besse P A, Popovic R S, Ribordy G and Gisin N 2003 *Rev. Sci. Instr.* **74** 3263

[46] Verevkin A et al. 2002 *Appl. Phys. Lett.* **80** 4687

[47] Korneev A et al. 2004 *Appl. Phys. Lett.* **84** 5338

[48] Dodonov A V, Mizrahi S S and Dodonov V V 2007 *Phys. Rev. A* **75** 013806

[49] Gardiner G W and Zoller P 2000 *Quantum Noise* (Springer-Verlag: Berlin)

[50] Plenio M B and Knight P L 1998 *Rev. Mod. Phys.* **70** 101

[51] Hadfield R H et al. 2005 *Opt. Expr.* **13** 10846

[52] Mandel L 1979 *Opt. Lett.* **4** 205

[53] Wiseman H M and Milburn G J 1993 *Phys. Rev. A* **47** 642